

Acknowledgment. This work was supported in part by the Office of Naval Research.

Registry No. 1, 80297-67-2; 2, 80297-88-7; 3, 80297-86-5; 4, 80297-87-6; 5, 80297-89-8; *cis*-6, 84624-30-6; *trans*-6, 84624-31-7; hexachlorocyclophosphazene, 940-71-6; hexafluorocyclophosphazene, 15599-91-4; methyl vinyl ether, 107-25-5; phenyl-

pentafluorocyclophosphazene, 2713-48-6; phenyllithium, 591-51-5; (dimethylamino)pentafluorocyclophosphazene, 23208-17-5; dimethylamine, 124-40-3; ethyl vinyl ether, 109-92-2.

Supplementary Material Available: Table I showing major mass spectral fragments and their relative intensities (6 pages). Ordering information is given on any current masthead page.

Contribution from the Laboratoire de Chimie Physique Organique, ERA CNRS 222, Université de Nancy I, 54506 Vandoeuvre-les-Nancy Cédex, France

Stereochemically Nonrigid Paramagnetic Tris Chelate Complexes of Cobalt(II) with Octamethylpyrophosphoramidate and Nonamethylimidodiphosphoramidate. An NMR Study

P. R. RUBINI, Z. POATY, J.-C. BOUBEL, L. RODEHÜSER, and J.-J. DELPUECH*

Received July 27, 1982

The terminal *N*-methyl substituents of the title ligands, OMPA and NIPA, are shown to be diastereotopic in the D_3 hexacoordinated complex ions $\text{Co}(\text{OMPA})_3^{2+}$ (**1**) and $\text{Co}(\text{NIPA})_3^{2+}$ (**2**), prepared as solutions of their perchlorates in a $\text{CD}_3\text{NO}_2/\text{CD}_2\text{Cl}_2$ solvent mixture. Contact and pseudocontact contributions to the isotropic shifts have been analyzed, with the assumption of a known geometry and identical contact shifts for both sets of diastereotopic protons. Ambiguities in line assignments are removed by a comparison of contact shifts in **1** and **2** and an examination of the temperature dependence of contact shifts and of paramagnetic line broadenings. Two types of exchange are revealed on raising the temperature from -20 to $+100$ °C: (i) an intramolecular optical inversion between the Δ and Λ enantiomers of **1** and **2** at the lower temperatures with $k_i(25$ °C) = 1.63×10^4 and 0.17×10^4 s $^{-1}$, ΔH_i^\ddagger = 13.5 and 10.9 kcal·mol $^{-1}$, and ΔS_i^\ddagger = 5.9 and -7.3 eu, respectively, and (ii) a bimolecular ligand exchange in complex **1** at the higher temperatures, with $k_e(25$ °C) = 3.80 s $^{-1}$ mol $^{-1}$ ·dm 3 , ΔH_e^\ddagger = 13.0 kcal·mol $^{-1}$, and ΔS_e^\ddagger = -12.4 eu. The rate-determining step for both processes involves the detachment of one end of one bidentate ligand from the metal atom to yield a pentacoordinated intermediate, which then either returns quickly to the initial complex molecule or to its enantiomer (optical inversion) or fastens a new ligand molecule from the bulk solution.

Introduction

In previous reports, $^{1-4}$ we have shown the possibility of using ^1H or ^{31}P DNMR to study the structure and dynamics of six-coordinate tris chelates of bivalent and trivalent diamagnetic cations with a diphosphorylated symmetrical bidentate ligand, nonamethylimidodiphosphoramidate (NIPA, $(\text{NMe}_2)_2\text{P}(\text{O})\text{NMeP}(\text{O})(\text{NMe}_2)_2$). An important feature of the ^1H spectra of these compounds is the existence of diastereotopic terminal *N*-methyl substituents, 1 as is expected for D_3 complexes. Solutions of D_3 tris chelates contain equal quantities of two chiral isomers, Δ and Λ , $^{5-7}$ which yield identical spectra. Within each isomer, the terminal *N*-methyl substituents are not mutually interchanged through any symmetry operation (C_3 , $3C_2$) of the D_3 symmetry point group. Two signals are therefore observed at low temperature ($T \approx -80$ °C) for the two nonequivalent *N,N*-dimethyl substituents $\text{N}(1)\text{Me}_2$ and $\text{N}(2)\text{Me}_2$ (Figures 1 and 3), attached to each phosphorus atom. At higher temperatures, optical inversion, $\Delta \rightleftharpoons \Lambda$, brings about a rapid interchange, $\text{N}(1)\text{Me}_2 \rightleftharpoons \text{N}(2)\text{Me}_2$, on the NMR time scale. However, the very small chemical shift differences between the diastereotopic protons in diamagnetic chelates, 1 e.g. $\Delta\delta = 0.01$, 0.004 , and 0.005 for $\text{Al}(\text{NIPA})_3^{3+}$, $\text{Ga}(\text{NIPA})_3^{3+}$, and $\text{In}(\text{NIPA})_3^{3+}$, respectively, prevent accurate measurements of the optical inversion rate.

Moreover the NMR window is so narrow that the exchange rate is immeasurably slow on the NMR time scale up to the boiling point of the solutions (for most trivalent cations) or immeasurably fast down to the freezing point of the solutions (for most divalent cations). Finally, no simple relationship can be found between the structure of the diamagnetic complexes and the value of the observed shifts $\Delta\delta$, thus preventing us from assigning individual resonances to the two sets of diastereotopic protons.

These difficulties prompted us to investigate paramagnetic cobalt(II) octahedral chelates where the triply degenerate $^4T_{1g}$ ground state is expected to produce magnetic anisotropy and significant dipolar shifts, 8 as was pointed out by La Mar for the (4,7-dimethyl-1,10-phenanthroline)bis(acetylacetonate)-cobalt(II) complex. 9 The octamethylpyrophosphoramidate ligand (OMPA, $(\text{NMe}_2)_2\text{P}(\text{O})-\text{O}-\text{P}(\text{O})(\text{NMe}_2)_2$) was preferred in a first step to the NIPA ligand, since only the crystal structure of the complex ion $\text{Co}(\text{OMPA})_3^{2+}$ is described in the literature. 10 The complexes $\text{Co}(\text{OMPA})_3^{2+}, 2\text{ClO}_4^-$ (**1**) and $\text{Co}(\text{NIPA})_3^{2+}, 2\text{ClO}_4^-$ (**2**) are prepared in the solid state $^{11-13}$ and are then dissolved in an inert solvent, either in pure nitromethane or in a 2:1 v/v mixture of methylene chloride and nitromethane (" C_2N "). Two lines are effectively obtained at low temperatures (-60 and -20 °C), one of which is located upfield and the second one downfield, by several ppm, with respect to the signal of a diamagnetic analogue, the complex ion 14 $\text{Mg}(\text{OMPA})_3^{2+}$. An inspection of the isotropic shifts and

(1) P. R. Rubini, L. Rodehüser, and J.-J. Delpuech, *Inorg. Chem.*, **18**, 2962 (1979).

(2) K. Bokolo, J.-J. Delpuech, L. Rodehüser, and P. R. Rubini, *Inorg. Chem.*, **20**, 992 (1981).

(3) L. Rodehüser, P. R. Rubini, K. Bokolo, and J.-J. Delpuech, *Inorg. Chem.*, **21**, 1061 (1982).

(4) P. R. Rubini, K. Bokolo, L. Rodehüser, and J.-J. Delpuech, *Nouv. J. Chim.*, **6**, 259 (1982).

(5) R. H. Holm in "Dynamic Nuclear Magnetic Resonance Spectroscopy", L. M. Jackman and F. A. Cotton, Eds., Academic Press, New York, 1975, Chapter 9.

(6) R. C. Fay and T. S. Piper, *J. Am. Chem. Soc.*, **85**, 500 (1963); *Inorg. Chem.*, **3**, 348 (1964).

(7) B. Jurado and S. Springer, *J. Chem. Soc. D*, 81 (1971).

(8) J. P. Jesson in "NMR of Paramagnetic Molecules", G. N. La Mar, W. D. Horrocks, and R. H. Holm, Eds., Academic Press, New York, 1973, Chapter 1.

(9) G. N. La Mar, *J. Am. Chem. Soc.*, **92**, 1806 (1970).

(10) M. D. Joesten, M. S. Hussain, and P. G. Lenhart, *Inorg. Chem.*, **9**, 151 (1970).

(11) M. D. Joesten and K. M. Nykerk, *Inorg. Chem.*, **3**, 548 (1964).

(12) K. P. Lannert and M. D. Joesten, *Inorg. Chem.*, **7**, 2048 (1968).

(13) M. W. G. De Bolster and W. L. Groeneveld, *Recl. Trav. Chim. Pays-Bas*, **91**, 171 (1972).

Table I. ^1H Paramagnetic Shifts δ_{p_1} and δ_{p_2} of the Diastereotopic Terminal *N*-Methyls of the Complex Ions $\text{Co}(\text{OMPA})_3^{2+}$ and $\text{Co}(\text{NIPA})_3^{2+}$ in a 2:1 v/v Mixture of Deuterated Dichloromethane and Nitromethane at Five Temperatures, the Corresponding Line Widths $\delta\nu_1$ and $\delta\nu_2$ (Hz), the Dissection of the Paramagnetic Shifts into a Common Contact Shift,^a and Two Different Pseudocontact Shifts δ_{pc_1} and δ_{pc_2} ^b

$T, ^\circ\text{C}$	δ_{p_1}	δ_{p_2}	$\delta\nu_1$	$\delta\nu_2$	$\delta_{c'}$	δ_c	δ_{cT}	δ_{pc_1}	δ_{pc_2}	
	$\text{Co}(\text{OMPA})_3^{2+}$									
-82.5	14.25	-7.63	76	126	1.20	5.42	1033	8.83	-13.05	
-68	13.86	-8.31	52.5	85	0.64	4.91	1007	8.95	-13.22	
-52	13.37	-8.79	42	60	0.15	4.42	977	8.95	-13.21	
-36	12.69	-8.87	20	35	-0.17	3.99	946	8.70	-12.86	
-21	11.93	-8.65			-0.34	3.62	913	8.31	-12.27	
	$\text{Co}(\text{NIPA})_3^{2+}$									
-78.5	25.82	-26.95	68	116	-5.65	4.52	880	21.30	-31.47	
-51	21.37	-22.31	67	94	-4.68	3.74	834	17.63	-26.05	
-43	19.69	-20.77	62	94	-4.41	3.38	778	16.31	-24.09	
-36	18.65	-19.47	44	69	-4.09	3.26	773	15.39	-22.73	
-26	17.49	-18.23	32	58	-3.82	3.07	759	14.42	-21.30	

^a $\delta_{c'}$ or δ_c according to two opposite line assignments; see text. ^b The validity of the Curie law for contact shifts is shown for convenience by displaying the product δ_{cT} (in ppm·K).

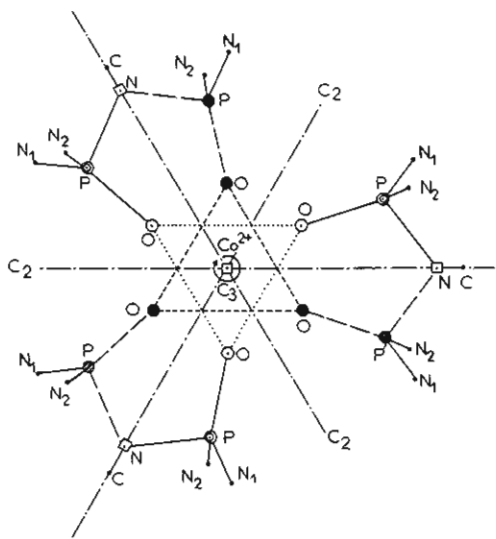


Figure 1. Projection of the complex $\text{Co}(\text{NIPA})_3^{2+}$ along the C_3 rotation axis showing the nonequivalence of the terminal nitrogen atoms N_1 and N_2 . Darkened symbols designate atoms above the mean molecular plane defined by the central ion Co^{2+} and the three bridging nitrogen atoms (open squares).

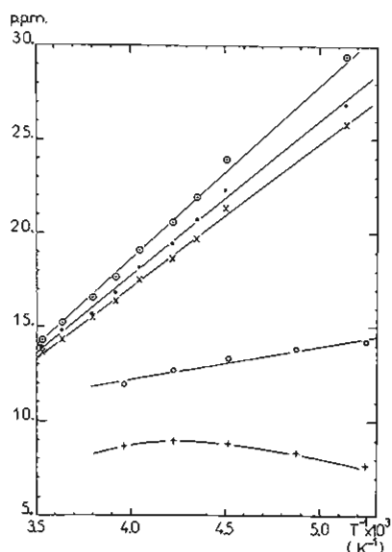


Figure 2. Temperature dependence of the methyl ^1H chemical shifts δ_{p_2} (●), δ_{p_1} (○), and $-\delta_{p_2}$ (×) for the NIPA ligand and δ_{p_1} (○) and $-\delta_{p_2}$ (+) for the OMPA ligand (for explanation of the δ values see text).

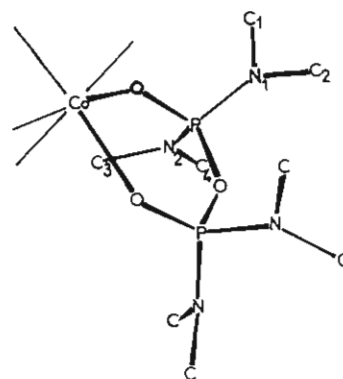


Figure 3. Partial view of the structure of the complex $\text{Co}(\text{OMPA})_3^{2+}$ in analogy to the X-ray structure from ref 10.

of the associated line widths allowed us to assign the low-field and high-field resonances to the methyl substituents of $N(1)$ and $N(2)$, respectively, with a good degree of certainty. Two dynamic processes were observed on raising the temperature, (i) the abovementioned optical inversion from ca. -20 to $+70$ $^\circ\text{C}$ and (ii) an intermolecular ligand exchange at higher temperatures (60 – 100 $^\circ\text{C}$) between coordinated OMPA molecules and free OMPA molecules (added in excess to a solution of the complex salt). These studies were extended in a second step to the case of NIPA, the study of the intermolecular exchange being impossible however because of a fortuitous coincidence of the two exchanging lines.

Experimental Section

Materials. Nonamethylimidodiphosphoramidate and octamethylpyrophosphoramidate have been synthesized by reported methods.^{1,15,16} The cobalt(II) complexes $\text{Co}(\text{OMPA})_3(\text{ClO}_4)_2$ (1) and $\text{Co}(\text{NIPA})_3(\text{ClO}_4)_2$ (2) were prepared in the solid state from the hydrated perchlorate $\text{Co}(\text{ClO}_4)_2 \cdot 6\text{H}_2\text{O}$ (Alfa Ventron) as described in a previous publication.¹ The solvents used in the experiments were CEA¹⁷ deuterated nitromethane and dichloromethane. All solutions were prepared by weight under purified argon in a glovebox.

NMR Spectroscopy. Proton spectra were taken on a 250-MHz Cemea spectrometer with Me_4Si as an internal reference. Chlorine-35 Fourier transform spectroscopy was performed on a Bruker WP-80 apparatus at 7.84 MHz. The unknown electron magnetic moment of $\text{Co}(\text{NIPA})_3(\text{ClO}_4)_2$ was measured according to the method of Evans,¹⁸ with a JEOL C60-HL apparatus working at 60 MHz. The

(14) G. Doucet Ladevèze, Thesis, Nancy, France, 1982.

(15) A. D. F. Toy and E. N. Walsh, *Inorg. Synth.*, 7, 73 (1963).

(16) M. W. G. De Bolster and W. L. Groeneveld, *Recl. Trav. Chim. Pays-Bas*, 90, 687 (1971).

(17) CEA, Service des Molécules Marquées, F-91190 Gif-sur-Yvette, France.

temperature in DNMR experiments was periodically checked with a thermometer immersed in the sample tube and was found constant within ± 0.5 °C.

Line-Shape Measurements. "Static" spectra, i.e. reference spectra without any exchange, were performed at a series of five temperatures from -80 to -35 °C (Table I). Protons in the bound ligand do not exhibit the usual coupling pattern:¹ the spectrum of each type of methyl is represented by a singlet in any case due to the fast paramagnetic relaxation of the phosphorus nuclei. Measuring the corresponding isotropic shifts allowed us to extrapolate the chemical shift differences between exchanging sites to any temperature. *The intramolecular exchange* due to optical inversion took place from -20 to $+70$ °C and from -5 to $+99$ °C for **1** and **2**, respectively, and is simply described by a two-line exchange between equally populated sites. The NMR rate constants thus determined, k_i (in s^{-1}), allowed us to extrapolate k_i for the higher temperatures required to study *the intermolecular exchange*. The latter exchange was investigated by adding known quantities C_f of free OMPA to the above solutions of the complexes at temperatures ranging from 60 to 96 °C. In fact both exchanges, intra- and intermolecular, are occurring under these conditions. A four-site exchange should therefore be used, between the two singlets (sites 1 and 2) representing the bound ligand (see above) and the doublet (sites 3 and 4) of the free ligand. Theoretical line shapes are computed by using a matrix formalism given by Anderson,¹⁹ Kubo,²⁰ and Sack²¹ and the program ECHGN.²² The appropriate exchange matrix is written as

$$\begin{array}{cccc} -(k_i + k) & k_i & k/2 & k/2 \\ k_i & -(k_i + k) & k/2 & k/2 \\ kr/2 & kr/2 & -kr & 0 \\ kr/2 & kr/2 & 0 & -kr \end{array}$$

with $r = C_b/C_f$ (C_b = concentration of the bound ligand, which is 3 times the concentration of the complex) and k , the intermolecular NMR rate exchange, to be determined. All calculations were performed on a Texas Instruments 980A minicomputer equipped with a Hewlett-Packard 7210A digital plotter.

Results and Discussion

Structure of the Complexes. The stoichiometry of complexes **1** and **2** in solution was checked by comparing the total line intensity of bound ligand molecules with that of a known quantity of free ligand added in excess. From the area ratio of the signals, coordination numbers of 6 ± 0.3 were effectively found for both complexes. The absence of perchlorate ions in the first coordination sphere of the Co^{2+} cation is shown by the fact that no splitting of the IR absorption line of the perchlorate ion at 616 cm^{-1} could be detected.^{13,23} Another evidence strongly supporting the absence of ionic association is the sharpness of the ^{35}Cl signal (~ 3.5 Hz), characteristic of the free perchlorate ion in a cubic nonparamagnetic environment. Finally, the D_3 symmetry of the complex was nicely confirmed by the presence of two signals for the terminal *N*-methyls, one of which (a_1) is located downfield (at δ_1) and the other one upfield (δ_2) with respect to the signal of a diamagnetic analogue, $Mg(OMPA)_3^{2+}$ or $Mg(NIPA)_3^{2+}$ (both at $\delta_D = 2.79$), itself very close to those of the free ligands, $\delta_f = 2.65$ or 2.66 , respectively.

Paramagnetic Shifts. Isotropic shifts are determined as the differences $\delta_{p_1} = \delta_1 - \delta_D$ and $\delta_{p_2} = \delta_2 - \delta_D$ at several temperatures in the no-exchange region (-80 to -20 °C). The reported values (Table I) show a strong dependence upon the temperature, which can be visualized on plots of δ_{p_1} , δ_{p_2} as functions of $1/T$ (Figure 2). Linear plots are obtained for the complex **2**

$$\delta_{p_1} = -13.815 + 7732.16/T \quad (1)$$

$$\delta_{p_2} = 15.425 - 8289.8/T \quad (2)$$

and for the low-field line of complex **1**

$$\delta_{p_1} = 5.075 + 1783.51/T \quad (3)$$

It may be noted that the slope of the last line is much weaker than that of lines for the NIPA complex and that the quality of the fit is rather poor (correlation coefficient of 0.9783 instead of 0.9991 and 0.9981), as shown by the slight curvature of the corresponding plot (Figure 2). This tendency to curvature is still more evident for the isotropic shift of the upfield signal of complex **1**, which clearly shows a maximum at -36 °C, first increasing and then decreasing in magnitude as the temperature is raised (instead of continuously decreasing as is observed for the other three lines). A linear plot is also obtained for the isotropic shift δ_{p_b} of the bridging *N*-methyl group of NIPA in complex **2**

$$\delta_{p_b} = -19.92 + 9635.15/T \quad (4)$$

All of these lines have a *nonzero intercept*. Different explanations for such a situation have been given in the literature such as ion-pairing or hydrogen-bonding interactions and temperature-dependent chemical equilibria, as pointed out by Perry and Drago.²⁴ These causes seem to be ruled out in the present case. In fact deviations from a Curie law are the general rule for cobalt(II) complexes, as pointed out by Jesson⁸ and McGarvey.²⁵ In the case of Co(II) poly(1-pyrazolyl)-borate complexes, these deviations were shown to arise from the pseudocontact and not from the contact shift contribution to the overall isotropic shift. We are therefore led to examine in the following a possible dissection of the observed paramagnetic shifts δ_{p_1} , δ_{p_2} , and δ_{p_b} into the above-mentioned contributions.

Analysis of Isotropic Shifts. As stated above, the isotropic shifts δ_{p_i} ($i = 1, 2$, or b) are the sum of contact and pseudocontact contributions, δ_{c_i} and δ_{pc_i} , respectively:

$$\delta_{p_i} = \delta_{c_i} + \delta_{pc_i} \quad (5)$$

In hexacoordinated Co(II) complexes, both contact and pseudocontact interactions make significant contributions to the observed paramagnetic shifts.⁸ The quantitative separation of dipolar and contact shifts is a difficult problem in this case, which is generally solved by evaluating either dipolar shifts from NMR or ESR data for complexes of known geometry or contact shifts calculated by quantum-mechanical methods.²⁶ In fact, quantum-mechanical calculations by ab initio methods are too complex for these large structures involving many atoms and too uncertain if one uses approximate semiempirical methods. Dipolar shifts can be estimated from the general formula⁸

$$\delta_{pc} = D(3 \cos^2 \theta - 1)/r^3 \quad (6)$$

where θ and r are the polar angle (with respect to the C_3 symmetry axis) and the length of the vector connecting the Co(II) atom to the examined proton, respectively, and

$$D = (\chi_{\parallel} - \chi_{\perp})/3 \quad (7)$$

χ_{\parallel} and χ_{\perp} are the unknown magnetic susceptibilities along the principal axes of the complex (the C_3 and C_2 axes, respectively). For freely rotating methylic protons, the term $(3 \cos^2 \theta - 1)/r^3$ must be averaged over all orientations. This term has been evaluated with use of the geometry of complex

(18) D. F. Evans, *J. Chem. Soc.*, 2003 (1959).

(19) P. W. Anderson, *J. Phys. Soc. Jpn.*, **9**, 316 (1954).

(20) R. Kubo, *J. Phys. Soc. Jpn.*, **9**, 935 (1954).

(21) R. A. Sack, *Mol. Phys.*, **1**, 163 (1958).

(22) M. L. Martin, J.-J. Delpeuch, and G. J. Martin, "Practical NMR Spectroscopy", Heyden, London, 1979, pp 441-444.

(23) C. Airoldi, Y. Gushikem, and C. R. Puschel, *J. Coord. Chem.*, **6**, 17 (1976).

(24) W. D. Perry and R. S. Drago, *J. Am. Chem. Soc.*, **93**, 2183 (1971).

(25) B. R. McGarvey, *J. Chem. Phys.*, **53**, 86 (1970).

(26) W. D. Horrocks in "NMR of Paramagnetic Molecules", G. N. La Mar, W. D. Horrocks, R. H. Holm, Eds., Academic Press, New York, 1973, Chapter 4.

Table II. Polar Coordinates (θ , r) and Geometric Factors for the Protons H_{ij}^a Situated on Carbons C_i ($i = 1-4$) in the Complex Ion $\text{Co}(\text{OMPA})_3^{2+}$

atom	θ , deg	r , Å	$10^{-3}(3 \cos^2 \theta - 1)/r^3$ Å ⁻³
H _{1,1}	68.84	5.115	-4.551
H _{1,2}	69.22	6.369	-2.409
H _{1,3}	58.20	5.488	-1.011
H _{2,1}	95.76	5.375	-6.226
H _{2,2}	89.32	5.855	-4.998
H _{2,3}	99.08	4.478	-10.304
H _{3,1}	63.75	5.877	-2.035
H _{3,2}	53.70	6.196	0.216
H _{3,3}	65.84	5.971	-2.336
H _{4,1}	33.30	4.830	9.725
H _{4,2}	47.65	4.555	3.828
H _{4,3}	29.78	3.332	34.195

^a For the notations, see the text and Figure 3.

1 in the solid state. X-ray crystallography¹⁰ yields the coordinates of the protons H_{ij} ($j = 1-3$) attached to carbons C_i ($i = 1-4$), themselves attached to either of the two diastereotopic nitrogens N(1) (carbons C_1 and C_2) or N(2) (carbons C_3 and C_4) (Figure 3). Structures in the solid state and in solutions of the complexes might differ slightly, but results show that the X-ray geometric parameters are a reasonable base for the calculations described in the following. The value $(3 \cos^2 \theta_{ij} - 1)/r_{ij}^3$ was computed for each proton H_{ij} (Table II), and two distinct averages may be computed for the diastereotopic sites N(1) and N(2) (eq 8 and 9, respectively) with

$$\langle (3 \cos^2 \theta - 1)/r^3 \rangle_1 = \sum_{i=1}^2 \sum_{j=1}^3 (3 \cos^2 \theta_{ij} - 1)/r_{ij}^3 = -4.916 \times 10^{-3} \text{ Å}^{-3} \quad (8)$$

$$\langle (3 \cos^2 \theta - 1)/r^3 \rangle_2 = \sum_{i=3}^4 \sum_{j=1}^3 (3 \cos^2 \theta_{ij} - 1)/r_{ij}^3 = 7.265 \times 10^{-3} \text{ Å}^{-3} \quad (9)$$

the assumption of free rotation around the C-H and N-C bonds between the positions H_{ij} found in the solid state. We may then compute the ratio of the terminal *N*-methyls of OMPA in complex **1**

$$\delta_{\text{pc}_1}/\delta_{\text{pc}_2} \text{ or } \delta_{\text{pc}_2}/\delta_{\text{pc}_1} = \frac{\langle (3 \cos^2 \theta - 1)/r^3 \rangle_1}{\langle (3 \cos^2 \theta - 1)/r^3 \rangle_2} \quad (10)$$

i.e. $\delta_{\text{pc}_1}/\delta_{\text{pc}_2} = -1.478$ or -0.677 , respectively. The above ambiguity arises from the unknown assignment of lines a_1 , a_2 to either N(1)Me₂, N(2)Me₂ or to N(2)Me₂, N(1)Me₂ substituents, respectively. We are then left with two problems: removing the above ambiguity and determining the dipolar shifts themselves. Approximate methods are used in general to solve this kind of problem. They have been examined in a review by Horrocks.²⁶ None of them are strictly applicable to the present complexes. However, some of these methods are pointing to the general procedure of comparing complexes with similar delocalization mechanisms, a basic concept we have extended to structural units contained within a given complex. This means that we have assumed identical delocalization mechanisms, and therefore identical contact shifts $\delta_{c_1} = \delta_{c_2}$, for the diastereotopic N(1)Me₂ and N(2)Me₂ groups in complex **1**. This seems to be a reasonable assumption on the basis of the local symmetry in the structural unit containing the Co(II) atom bonded to one bidentate ligand. This assumption allows us to recast eq 10 into the form

$$\frac{\delta_{\text{p}_1} - \delta_{c'}}{\delta_{\text{p}_2} - \delta_{c'}} = -1.478 \quad \text{or} \quad \frac{\delta_{\text{p}_1} - \delta_c}{\delta_{\text{p}_2} - \delta_c} = -0.677 \quad (11)$$

where δ_c and $\delta_{c'}$ are the common contact shift values $\delta_{c_1} = \delta_{c_2}$,

Table III. ¹H Paramagnetic Shifts δ_{pb} of the Bridging *N*-Methyl in the Complex Ion $\text{Co}(\text{NIPA})_3^{2+}$ as a Function of the Temperature and the Corresponding Pseudocontact, δ_{pc_b} , and Contact Shifts, $\delta_{c'_b}$ or δ_{c_b} , according to Two Opposite Line Assignments^a

	T , °C					
	-78.5	-51	-43	-36	-26	-10
δ_{pb}	29.50	23.88	21.88	20.54	19.02	16.54
δ_{pc_b}	± 24.81	± 20.54	± 19.00	± 17.93	± 16.80	± 14.62
$\delta_{c'_b}$	54.31	44.42	40.88	38.47	35.82	31.16
δ_{c_b}	4.69	3.34	2.88	2.61	2.22	1.92
$\delta_{c_b} T$, ppm·K	913	742	663	619	549	505

^a See text.

depending on whether the low-field or the high-field signal is assigned to the N(1)Me₂ substituent. The δ_c , $\delta_{c'}$ values computed according to eq 11 are reported in Table I.

Similar calculations were performed (Table I) for the NIPA complex **2**, with the supplementary assumption of identical geometries for complexes **1** and **2**. (The crystal structure of hexacoordinated NIPA complexes has not been described to date; however, they are reported to be isomorphous²⁷ with the OMPA complexes of known structure.¹⁰) The dipolar shift δ_{pc_b} , and therefore the contact shift $\delta_{c_b} = \delta_{\text{pb}} - \delta_{\text{pc}_b}$, of the bridging *N*-methyl in the NIPA complex **2** can be in turn computed by using an equation²⁸ analogous to eq 10:

$$\frac{\delta_{\text{pc}_1}}{\delta_{\text{pc}_b}} = \frac{\langle (3 \cos^2 \theta - 1)/r^3 \rangle_1}{\langle (3 \cos^2 \theta - 1)/r^3 \rangle_b} \quad (12)$$

Two sets of values, δ_{pc_b} and $\delta_{c'}$ or δ_c , are obtained according to the above two opposite line assignments (Table III).

The remaining ambiguity can be removed by an inspection of the two sets of contact shifts. First, $\delta_{c'}$ values in complex **1** do not follow even an approximate Curie law, since their sign changes from positive to negative over the temperature range investigated (Table I). Second, contact shifts $\delta_{c'}$ are widely different for complexes **1** and **2**, a fact quite unexpected for so closely related structures. Finally, contact shifts δ_{c_b} for the bridging *N*-methyl of complex **2** are large and positive, while those for the terminal *N*-methyls, $\delta_{c'}$, are negative and smaller by an order of magnitude. The results that are expected normally, however, are obtained if contact shifts δ_c and δ_{c_b} are taken into consideration. This set of values will therefore be adopted in the following, together with the corresponding pseudocontact shift values δ_{pc_1} , δ_{pc_2} , and δ_{pc_b} reported in Tables I and III. This means that the low-field singlet a_1 should be assigned to the N(1)Me₂ substituents (carbons 1 and 2), defined by the data of Table II (cf. Figure 3).

We may then compute the difference $\Delta\chi = \chi_{\perp} - \chi_{\parallel}$ between transverse and longitudinal magnetic susceptibilities from eq 6 and 7, using the data of Table I. We may also estimate the mean value $\langle \chi \rangle = (\chi_{\parallel} + 2\chi_{\perp})/3$ from the measurement of the electronic moment μ ($\mu = 5.24^{11}$ and $5.08 \mu_B$ for complexes **1** and **2**, respectively) and the equation⁸

$$\mu^2 = 3k_B T \langle \chi \rangle \quad (13)$$

(27) P. T. Miller, P. G. Lenhart, and M. D. Joesten, *Inorg. Chem.*, **11**, 2221 (1972).

(28) The geometrical factor $(3 \cos^2 \theta - 1)/r^3$ in eq 13 was estimated by assuming distances $r_{\text{Co(II)-N}} = 3.592$ Å, $r_{\text{N-C}} = 1.450$ Å, and $r_{\text{C-H}} = 1.07$ Å equal to the Co(II)···O, N-C, and C-H distances in complex **1**, and an entirely free rotation of the methylic protons about the C_2 axis bearing the N-C bond (Figure 1), so that $r_{\text{Co(II)-H}} = 5.493$ Å and

$$\langle (3 \cos^2 \theta - 1)/r^3 \rangle = \left[\frac{3}{2} \left(\frac{r_{\text{C-H}} \sin 109^\circ 45'}{r_{\text{Co(II)-H}}} \right)^2 - 1 \right] / r_{\text{Co(II)-H}}^3 = -5.729 \times 10^{-3} \text{ Å}^{-3}$$

Table IV. Magnetic Susceptibilities of Complexes 1 and 2 (in 10^{-3} \AA^3)

$T, ^\circ\text{C}$	$\Delta\chi$	$\langle\chi\rangle$	χ_{\parallel}	χ_{\perp}
Co(OMPA) ₃ ²⁺				
-82.5	5.39	29.9	26.3	31.7
-68	5.46	27.8	24.2	29.7
-52	5.46	25.8	22.2	27.7
-36	5.31	24.0	20.5	25.8
-21	5.07	22.6	19.2	24.3
Co(NIPA) ₃ ²⁺				
-78.5	13.00	27.53	18.9	31.9
-51	10.76	24.12	16.9	27.7
-43	9.96	23.21	16.6	26.6
-36	9.39	22.60	16.3	25.7
-26	8.80	21.68	15.8	24.6

where $k_B = 1.3805 \times 10^{-16} \text{ erg}\cdot\text{K}^{-1}$ is the Boltzmann constant. The individual susceptibilities χ_{\perp} and χ_{\parallel} have been extracted from $\Delta\chi$ and $\langle\chi\rangle$ and are reported in Table IV. For a complex with only one thermally populated multiplet with effective spin S' , it is possible to compute the corresponding values of the g tensor⁸

$$g_{\parallel}^2 \text{ (or } g_{\perp}^2) = 3k_B T \chi_{\parallel} \text{ (or } \chi_{\perp}) / \beta^2 S'(S' + 1) \quad (14)$$

where β is the Bohr magneton.

However, such a simplified picture is not valid for a d^7 octahedral high-spin configuration, for which the complete Van Vleck equation has to be used.^{8,25} This is shown by strong deviations of the dipolar shifts from a Curie law, since a flat maximum of δ_{pc1} , δ_{pc2} as a function of the temperature is even observed for complex 1. A thorough calculation of the g tensor from the observed paramagnetic shifts would require the knowledge of the energy levels of the 12-fold degenerated $^4T_{1g}$ manifold.⁸

Paramagnetic Line Broadening. Another piece of evidence supporting the assignment of lines a_1 and a_2 is brought about by an examination of paramagnetic line broadenings $\delta\nu_1$ and $\delta\nu_2$ in complexes 1 and 2. The inequality $\delta\nu_1 < \delta\nu_2$ is of importance in this respect. Scalar and dipolar contributions, $(1/T_2)_{RS}$ and $(1/T_2)_{DD}$, to the transverse relaxation rate $1/T_2$ may be roughly estimated by using the simple model of an electron spin S with an isotropic g tensor and no zero-field splitting. These assumptions allow us to derive an isotropic hyperfine coupling A of 18.24 or 13.44 kHz from the approximate Curie law²⁹

$$\delta_c T = K_c = 2\pi A \mu(S(S+1))^{1/2} / 3k_B \gamma_H \quad (15)$$

where $K_c = (974 \pm 37) \times 10^{-6}$ and $(804 \pm 41) \times 10^{-6} \text{ ppm}\cdot\text{K}$, for complexes 1 and 2, respectively, and γ_H is the gyromagnetic ratio of the proton. The scalar contribution to relaxation³⁰ is then estimated according to the equation

$$(1/T_2)_{RS} = K_{RS} T_{1e} \quad (16)$$

and $K_{RS} = [8\pi^2 A^2 S(S+1)]/3 = 3.28 \times 10^{10}$ and $2.38 \times 10^{10} \text{ s}^{-2}$ for complexes 1 and 2, respectively, with the assumption of extreme narrowing conditions and a nuclear correlation time equal to the electronic relaxation time $T_{1e} \approx T_{2e}$. The dipolar contribution^{31,32} is computed according to the equations

$$(1/T_2)_{DD} = 10K_{DD} T_{1e} \quad K_{DD} = \frac{2}{15} \frac{\mu^2 \gamma_H^2 \beta^2}{\langle r^6 \rangle} \quad (17)$$

Table V. Rate Constants and Activation Parameters for Optical Isomerization in the Complex Co(OMPA)₃²⁺

$10^2 k_i, \text{ s}^{-1}$	$T, ^\circ\text{C}$							
	-21	-14.5	-6	+3	+44.5	+52	+61	+70
1.80	5.10	11.0	25.0	800	1200	2100	3400	
$k_i(25^\circ\text{C}) = 1.63 \times 10^4 \text{ s}^{-1}$, $\Delta H_i^\ddagger = 13.5 \pm 0.6 \text{ kcal}\cdot\text{mol}^{-1}$, $\Delta S_i^\ddagger = 5.9 \pm 2.0 \text{ cal}\cdot\text{mol}^{-1}\cdot\text{K}^{-1}$								

Table VI. Rate Constants and Activation Parameters for Optical Isomerization in the Complex Co(NIPA)₃²⁺

$T, ^\circ\text{C}^a$	$10^2 k_i, \text{ s}^{-1}^a$	$T, ^\circ\text{C}^b$	$10^2 k_i, \text{ s}^{-1}^b$
-5	1.50	-5	1.40
+2	3.50	+2	3.90
+10	7.50	+13	8.00
+20	17.0	+75	350
+87	425	+86	450
+99	700	+92	575
		+97	700

$$k_i(25^\circ\text{C}) = 1.70 \times 10^3 \text{ s}^{-1}$$
, $\Delta H_i^\ddagger = 10.9 \pm 0.5 \text{ kcal}\cdot\text{mol}^{-1}$,
 $\Delta S_i^\ddagger = -7.3 \pm 2 \text{ cal}\cdot\text{mol}^{-1}\cdot\text{K}^{-1}$

^a At $C_{\text{complex}} = 0.1 \text{ M}$. ^b At $C_{\text{complex}} = 0.2 \text{ M}$.

The mean value $\langle 1/r^6 \rangle$ is computed from the data of Table II for each of the two nonequivalent terminal N -methyls $N(1)\text{Me}_2$ and $N(2)\text{Me}_2$, $\langle 1/r^6 \rangle = 4.96 \times 10^{-5}$ and $16.42 \times 10^{-5} \text{ \AA}^{-6}$, respectively. This allows us in turn to estimate the two values $K_{DD} = 1.12 \times 10^{13}$ and $3.70 \times 10^{13} \text{ s}^{-2}$ for complex 1 and $K_{DD} = 1.05 \times 10^{13}$ and $3.48 \times 10^{13} \text{ s}^{-2}$ for complex 2. It is evident that scalar relaxation is negligible compared to dipolar relaxation. Under these conditions, the low-field singlet should be larger than the high-field line, the ratio of the line widths being the ratio of the respective K_{DD} values, i.e. 3.30 for both 1 and 2. In fact, the experimental ratio is only 1.60 ± 0.10 for both complexes over the temperature range investigated, presumably on account of the oversimplified model that has been used. It is, however, rewarding that the inequality $\delta\nu_1 < \delta\nu_2$ shows effectively the expected order. The electronic relaxation times T_{1e} , computed from eq 17, have indeed an expected order of magnitude for cobalt(II) complexes,^{33,34} e.g. $T_{1e} = 5.62 \times 10^{-13}$ and $2.97 \times 10^{-13} \text{ s}$ for complex 1 at -36°C (two values are obtained, one for each K_{DD} value).³⁵

Another interesting sequence is obtained when the line width of the bridging N -methyl, $\delta\nu_b$, is taken into consideration

$$\delta\nu_b < \delta\nu_1 < \delta\nu_2$$

e.g. at -36°C : $\delta\nu_b = 34 \text{ Hz}$, against $\delta\nu_1$ and $\delta\nu_2 = 44$ and 69 Hz , respectively. This is in line with a negligible scalar relaxation ($K_c = (665 \pm 108) \times 10^{-6} \text{ ppm}\cdot\text{K}$, $A = 12.85 \text{ kHz}$, and $K_{RS} = 1.63 \times 10^{10} \text{ s}^{-2}$) and a predominant dipolar relaxation with a coefficient $K_{DD} = 7.70 \times 10^{12} \text{ s}^{-2}$, which is effectively smaller than those values obtained for the low-field terminal N -methyls ($K_{DD} = 1.05 \times 10^{13} \text{ s}^{-2}$). The ratio of the corresponding K_{DD} values is even closer to the ratio of the experimental line widths, 1.36 against 1.30, than that mentioned above for the terminal N -methyls. This again confirms the assignment of lines a_1 and a_2 .

Rate of Optical Inversion. As the exchanging sites a_1 and a_2 are widely apart from each other, line shapes can be usefully studied over two distinct temperature ranges corresponding to (i) either the *slow-exchange region*, from -21 to $+3^\circ\text{C}$ for

(29) N. Bloembergen, *J. Chem. Phys.*, **27**, 595 (1957).
 (30) A. Abragam, "Principles of Nuclear Magnetism", Oxford University Press, London, 1961, p 289.
 (31) N. Bloembergen, E. M. Purcell, and R. V. Pound, *Phys. Rev.*, **73**, 679 (1948).
 (32) M. Rubinstein, A. Baram, and Z. Luz, *Mol. Phys.*, **20**, 67 (1971).

(33) N. Bloembergen and L. O. Morgan, *J. Chem. Phys.*, **34**, 842 (1961).
 (34) J.-C. Boubel and J.-J. Delpuech, *Mol. Phys.*, **27**, 113 (1974).
 (35) In fact, the extreme narrowing condition $\omega_e^2 T_{1e}^2 \ll 1$, where $\omega_e = 1.033 \times 10^{12} \text{ rad}\cdot\text{s}^{-1}$, is not fulfilled in the present case, so that the equation $1/T_{1e} = K_{DD}[3.5 + 6.5/(1 + \omega_e^2 T_{1e}^2)]T_{1e}$ should be used instead of eq 18, and $T_{1e} = 3.17 \times 10^{-13}$ and $7.28 \times 10^{-13} \text{ s}$, respectively.

Table VII. Rate Constants and Activation Parameters for Ligand Exchange on the Complex Ion $\text{Co}(\text{OMPA})_3^{2+}$

$T, ^\circ\text{C}$	$k_{\text{NMR}}, \text{s}^{-1}$		$k_e = k_{\text{NMR}}/C_{\text{ligand}}$ $\text{s}^{-1}\cdot\text{mol}^{-1}\cdot\text{dm}^3$	
	a	b	a	b
61.1	6.0	10	55	42
70.7	9.0	16	83	67
78.2	13	24	120	100
85.6	24	36	221	150
96.4	40	70	369	292

$$k_e(25^\circ\text{C}) = 3.80 \pm 0.5 \text{ s}^{-1}\cdot\text{mol}^{-1}\cdot\text{dm}^3, \Delta H^\ddagger_e = 13.0 \pm 0.6 \text{ kcal}\cdot\text{mol}^{-1}, \Delta S^\ddagger_e = -12.4 \pm 2 \text{ cal}\cdot\text{mol}^{-1}\cdot\text{K}^{-1}$$

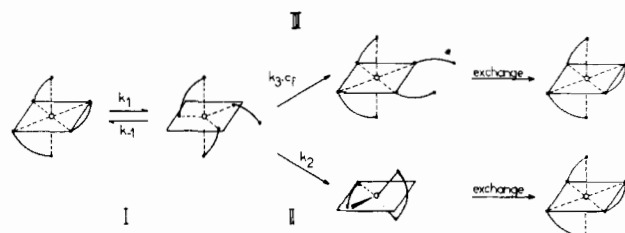
^a At $C_{\text{complex}} = 0.150 \text{ M}$ and $C_{\text{ligand}} = 0.108 \text{ M}$. ^b At $C_{\text{complex}} = 0.150 \text{ M}$ and $C_{\text{ligand}} = 0.239 \text{ M}$.

complex **1** and from -5 to $+20^\circ\text{C}$ for **2**, or (ii) *the fast-exchange-region*, from 44 to 70°C , and from 87 to 99°C for **1** and **2**, respectively (no signal can be distinguished from the base line noise around coalescence). These peculiarities allowed us to explore a large range of temperatures, leading to a high degree of accuracy in determining the activation parameters, $\Delta H^\ddagger_i = 13.5 \pm 0.6$ and $10.9 \pm 0.5 \text{ kcal}\cdot\text{mol}^{-1}$ and $\Delta S^\ddagger_i = 5.9 \pm 2.0$ and $-7.3 \pm 2.0 \text{ cal}\cdot\text{mol}^{-1}\cdot\text{K}^{-1}$, and in interpolating the intramolecular rate constant at 25°C , $k_i = 1.63 \times 10^4$ and $0.170 \times 10^4 \text{ s}^{-1}$, for complexes **1** and **2**, respectively (Tables V and VI). In the low-temperature region, line shapes are not altered by adding free ligand to the solutions of the complexes, and the NMR exchange rates were found to be also independent of the salt concentration (Table VI). This readily allowed us to assess that a pure *intramolecular process* is responsible for the ligand rearrangement leading to optical inversion.

Ligand Exchange. At higher temperatures, a second NMR site exchange takes place between the collapsed lines of complex **1** and the signal of free OMPA, revealing an intermolecular ligand exchange between the first coordination sphere and the ligand molecules in the bulk solution. Kinetic measurements using two concentrations, C_f , of added free ligand show that the exchange rate is approximately proportional to C_f . The kinetic law for the ligand-exchange process is therefore first order with respect to C_f , in contrast with the results obtained for the intramolecular process. Taking spectra at several temperatures allowed us to derive activation parameters, $\Delta H^\ddagger_e = 13.0 \pm 0.6 \text{ kcal}\cdot\text{mol}^{-1}$ and $\Delta S^\ddagger_e = -12.4 \pm 2.0 \text{ cal}\cdot\text{mol}^{-1}\cdot\text{K}^{-1}$, and to extrapolate the ligand-exchange rate constant at 25°C , $k_e = 3.80 \text{ s}^{-1}\cdot\text{mol}^{-1}\cdot\text{dm}^3$ (Table VII). Similar measurements were not feasible for the NIPA complex with a sufficient degree of accuracy, because the signal of free NIPA is very close to the center of lines a_1 and a_2 .

Mechanisms of Racemization and Ligand Exchange. The kinetic parameters for the *ligand exchange* in complex **1** are quite similar to those obtained for the complex of a diamagnetic cation, $\text{Mg}(\text{OMPA})_3^{2+}$, with the same ionic charge and a similar ionic radius (0.66 compared to 0.72 \AA): $k_e(25^\circ\text{C})$, ΔH^\ddagger_e , and ΔS^\ddagger_e are equal respectively to $4.5 \text{ s}^{-1}\cdot\text{mol}^{-1}\cdot\text{dm}^3$, $11.7 \text{ kcal}\cdot\text{mol}^{-1}$, and $-16.4 \text{ cal}\cdot\text{mol}^{-1}\cdot\text{K}^{-1}$ for the Mg complex against $3.8 \text{ s}^{-1}\cdot\text{mol}^{-1}\cdot\text{dm}^3$, $13.0 \text{ kcal}\cdot\text{mol}^{-1}$, and $-12.4 \text{ cal}\cdot\text{mol}^{-1}\cdot\text{K}^{-1}$. This similarity is in line with the generally accepted view that octamethylpyrophosphoramidate is an extremely weak-field ligand and that the metal-to-ligand bond is mainly ionic in character.^{10,36-38}

The fact that the racemization rate is much larger than the exchange rate—by three orders of magnitude for a 1 M so-

**Figure 4.** Reaction pathways (schematic) for the intra- and intermolecular exchanges on the tris-bidentate Co^{2+} complexes.

lution (as shown by the ratio $R = k_e C_f / k_i = 4.2 \times 10^3$ at 25°C)—confirms the presence of an *intramolecular process for optical inversion*, as already pointed out³⁹ in the case of the tris(1,10-phenanthroline) complexes of iron(II) and nickel(II). However, various internal rearrangements have been proposed to account for the racemization of octahedral complexes.^{5,40} The inversion may proceed by either of two general types of reaction pathways, the so-called twist mechanism, rhombic or trigonal, or the bond rupture mechanism (TBP transition state of Gordon and Holm⁴¹). These pathways may be unambiguously distinguished on stereochemical grounds⁵ in the case of dissymmetric bidentate ligands forming optically active cis and trans isomers. This possibility is ruled out in the case of complexes **1** and **2**, where symmetric ligands are involved.

In fact, many six-coordinate tris chelates are stereochemically labile and it is probable that rearrangements for the majority of these chelates occur by an internal dissociative pathway involving a five-coordinate species (Figure 4) with one of the chelate ligands bound as a unidentate ligand. Such an intermediate state should also represent the first step of the ligand-exchange process, as described in Figure 4. Evidence supporting this view is the general parallelism observed between optical inversion and ligand-exchange rates in NIPA or OMPA complexes.¹

We had already noticed that inversion is fast (slow) on the NMR time scale for NIPA complexes of diamagnetic cations which rapidly (slowly) exchange bound ligands with bulk ligand molecules. For example, trivalent ions such as Al^{3+} , Ga^{3+} , and In^{3+} , for which no intermolecular exchange of their NIPA ligands occurs up to the boiling point of the solvents used ($\sim 120^\circ\text{C}$) show also closely spaced singlets a_1, a_2 , which are observed even at room temperature.¹ For complexes of diamagnetic divalent cations such as $\text{Mg}(\text{NIPA})_3^{2+}$, which quickly exchange their ligands at temperatures of 60 – 100°C , separate lines a_1, a_2 can be obtained only at low temperatures ($\sim -60^\circ\text{C}$).¹ The cobalt(II) complex of OMPA, which suffers ligand exchange over a similar temperature range, effectively shows no optical inversion at -60°C . Investigations are in progress in our laboratory to measure inversion rates on trivalent ion complexes of OMPA such as $\text{Ga}(\text{OMPA})_3^{3+}$ and $\text{In}(\text{OMPA})_3^{3+}$. These investigations show indeed a sharp decrease of the racemization rate, by eight and two orders of magnitude, respectively, compared to that of $\text{Co}(\text{OMPA})_3^{2+}$. These facts strongly suggest the formation, in an initial step (I), of a TBP pentacoordinated intermediate common to both the optical inversion and ligand-exchange processes (Figure 4). The intramolecular return from the TBP intermediate to the initial complex molecule or to its enantiomer (rate constant k_{-1}) would compete with the attachment of the free end of an external ligand molecule (mechanism III, rate constant k_3) or with the release of both ends of one chelate molecule (mechanism II, rate constant k_2) to yield a tetracoordinated D_{2d} intermediate that is rapidly substituted by an external

(36) G. M. Woltermann and R. J. Wasson, *Chem. Phys. Lett.*, **16**, 92 (1972); *J. Magn. Reson.*, **9**, 486 (1973).

(37) R. A. Palmer and C. R. Taylor, *Inorg. Chem.*, **10**, 2546 (1971).

(38) R. S. Evans, A. F. Schreiner, M. C.-L. Yang, and R. A. Palmer, *Inorg. Chem.*, **15**, 3164 (1976).

(39) E. L. Blinn and R. G. Wilkins, *Inorg. Chem.*, **15**, 2952 (1976).

(40) F. Basolo and R. G. Pearson, "Mechanisms of Inorganic Reactions", Wiley, New York, 1958, Chapter 4.

(41) J. G. Gordon and R. H. Holm, *J. Am. Chem. Soc.*, **92**, 5319 (1970).

ligand molecule. Under these conditions¹

$$k_i = k_1/2 \quad (18)$$

and

$$k_{\text{NMR}}(\text{ligand exchange}) = \frac{k_1(k_2 + k_3C_f/2)}{k_{-1} + k_2 + k_3C_f} \quad (19)$$

A first-order or a second-order kinetic law for ligand exchange may be obtained as limiting forms of eq 19, depending on the complex investigated.¹ A second-order kinetic law $k_{\text{NMR}} = k_e C_f$ is observed in the present case, requiring $k_2 \ll k_3 C_f \ll k_{-1}$ and $k_e = k_1 k_3 / 2 k_{-1}$. Under these assumptions, $k_1(25^\circ\text{C}) = 3.2 \times 10^4$ and $3.4 \times 10^3 \text{ s}^{-1}$ for complexes **1** and **2** and $R = k_i/k_e = k_{-1}/k_3 = 4.29 \times 10^3$ for complex **1** at 25°C . The value of R shows that the internal reattachment of one ligand molecule to the TBP intermediate is 4.29×10^3 times more probable than the addition of a ligand molecule from the bulk solvent. The nearly equal values of the activation enthalpies ΔH_i^\ddagger and ΔH_e^\ddagger for complex **1** suggest a common energy barrier due to the bond-rupture step. In contrast, the activation entropies ΔS_i^\ddagger and ΔS_e^\ddagger are widely different. The positive value $\Delta S_i^\ddagger = 6 \text{ eu}$ is in line with an expected release of the steric strain in the pentacoordinate intermediate. The negative value $\Delta S_e^\ddagger = -12 \text{ eu}$ shows, according to eq 19, that the entropy loss in the bimolecular step (III) should outweigh by ca. -18 eu the entropy loss in the internal return process. A point that remains unexplained is the negative value $\Delta S_i^\ddagger = -7.3 \text{ eu}$ obtained for complex **2**. A negative value $\Delta S_i^\ddagger = -29.5 \text{ eu}$ is also obtained for the racemization of the tris(1,10-phenanthroline)cobalt(II) complex from the kinetic data reported in the literature³⁹ ($k_i = 6.9 \text{ s}^{-1}$ and $\Delta H_i^\ddagger = 7.5 \text{ kcal}\cdot\text{mol}^{-1}$ at 25°C), while the corresponding ΔS_e^\ddagger value is

positive: $\Delta S_e^\ddagger = 5.6 \text{ eu}$, $k_e(25^\circ\text{C}) = 0.16 \text{ s}^{-1}$, and $\Delta H_e^\ddagger = 20.2 \text{ kcal}\cdot\text{mol}^{-1}$. Further studies are therefore necessary to elucidate the problem of the signs and magnitudes of entropy variations in these processes.

Conclusions

There is a paucity of kinetic data on the racemization of optically active coordination compounds, since they often racemize very rapidly, so that a prior resolution into the pure enantiomers is not possible. This drawback can be circumvented by DNMR methods, which detect the exchange of diastereotopic nuclei between the Δ and Λ enantiomers at equilibrium. Although already described for some specific examples, the NMR methods seem to have never been applied to the archetypal case of paramagnetic trigonal tris chelates of transition-metal ions with three identical symmetric bidentate ligands. The above experiments show that a wealth of information can be obtained by using for this purpose bidentate phosphoramidate ligands, due to the magnetic nonequivalence of the two nitrogen atoms in the neighborhood of each phosphorus nucleus and to appropriate isotropic shifts. This is an additional feature of these powerful chelating reagents¹ that makes them very attractive as probes for the study of optical inversion processes in metal ion complexes.

Acknowledgment. Financial support from the Centre National de la Recherche Scientifique is gratefully acknowledged. All NMR spectra were recorded on spectrometers of the Groupement Régional de Mesures Physiques de l'Académie de Nancy-Metz. We thank M. Diter and Mrs. Eppiger for their technical assistance.

Registry No. **1**, 26167-79-3; **2**, 21665-90-7; octamethylpyrophosphoramidate, 152-16-9; nonamethylimidodiphosphoramidate, 34834-03-2.

Contribution from the Department of Chemistry, Purdue University, West Lafayette, Indiana 47907

Diosmium(IV) Complexes Containing Oxide and Carboxylate Bridges and a Weak Os-Os Interaction: Structure of (μ -Oxo)bis(μ -acetato)bis[dichloro(triphenylphosphine)osmium(IV)] as Its Diethyl Ether Solvate

JOHN E. ARMSTRONG, WILLIAM R. ROBINSON, and RICHARD A. WALTON*

Received June 14, 1982

The reactions of *trans*-OsO₂X₂(PR'₃)₂ (X = Cl or Br; PR'₃ = PPh₃ or PET₂Ph) with refluxing carboxylic acids have produced a new class of diosmium(IV) complexes of the type Os₂(μ -O)(μ -O₂CR)₂X₄(PR'₃)₂ (R = CH₃ or C₂H₅). The cyclic voltammograms of these complexes show a one-electron reduction with $E_{1/2}$ values in the range +0.09 to +0.23 V vs. SCE and an irreversible one-electron reduction between -0.79 and -1.01 V. Chemical reduction of Os₂(μ -O)(μ -O₂CCH₃)₂Cl₄(PPh₃)₂ using sodium metal has led to isolation of the Ph₄As⁺ salt of the monoanion. Other characterizations of the diosmium(IV) complexes have included ¹H NMR, IR, electronic absorption, and magnetic moment measurements and X-ray photoelectron spectroscopy. The X-ray crystal structure of the diethyl ether solvate of Os₂(μ -O)(μ -O₂CCH₃)₂Cl₄(PPh₃)₂ has been determined. This molecule is the only known example of a diosmium complex containing a single bent bridging oxide ligand. Besides the bridging oxide ligand, two distorted acetate ligands bridge the long Os-Os distance of 3.440 (2) Å. The distorted-octahedral coordination polyhedron about each Os atom is completed by two Cl atoms and a Ph₃P ligand. The diethyl ether molecule is disordered in the unit cell. The crystals belong to space group *P2₁/c* with $a = 13.066$ (3) Å, $b = 18.124$ (3) Å, $c = 19.619$ (4) Å, $\beta = 107.10$ (2)°, $V = 4441$ Å³, and $Z = 4$. The structure was solved by the heavy-atom method and refined by full-matrix least-squares procedures with anisotropic temperature factors to $R = 0.044$ for 4668 observed reflections.

Introduction

Although there are many osmium complexes containing [Os(μ -N)Os] and [Os(μ -O)₂Os] bridges,¹ compounds with a single Os-O-Os unit are rare. Notable exceptions are the

oxyhalo anions of osmium(IV) of the type [Os₂(μ -O)X₁₀]⁴⁻, but only in the case of Cs₄Os₂(μ -O)Cl₁₀ has this been documented by a crystal structure determination.² In the course of investigating the reactions of *trans*-OsX₄(PPh₃)₂ and

(1) See, e.g.: Gmelin, "Handbuch der Anorganischen Chemie"; Springer-Verlag: New York, 1980; Osmium Supplement, Vol. 1.

(2) Tebbe, K. F.; Von Schnering, H. G. Z. Anorg. Allg. Chem. 1973, 396, 66.